Supporting Information

Nonacyclic carbazole-based non-fullerene acceptors enables over 12% efficiency with enhanced stability for organic solar cells

Hongtao Wang[a], Zhuohan Zhang[b], Jiangsheng Yu[a], Xin Liu[a], Shenya Qu[a], Shun Guang[a], and Weihua Tang[b*]*

[a] *MIIT Key Laboratory of Advanced Solid Laser, Nanjing University of Science and Technology, Nanjing 210094, P. R. China*

[b] *School of Chemical Engineering, Nanjing University of Science and Technology, Nanjing 210094, P. R. China*

[*]*Corresponding authors. E-mail: yjs@njust.edu.cn; whtang@njust.edu.cn*

1. Materials and Synthesis

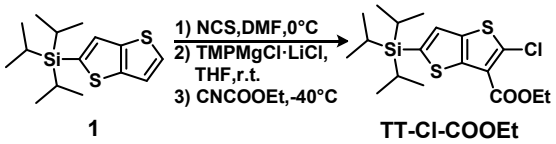

Scheme S1. Synthetic route of TT-Cl-COOEt.

Synthesis of **Ethyl 2-chloro-5-(triisopropylsilyl)thieno[3,2-*b*]thiophene-3-carboxylate(TT-Cl-COOEt)**

Compound triisopropyl(thieno[3,2-*b*]thiophen-2-yl)silane (4.0 g, 13.49 mmol) was dissolved in DMF (40 mL) at room temperature. *N*-Chlorosuccinimide (2.2 g, 16.19 mmol) was added and stirred at 50 ℃ for 24 h. The mixture was quenched by water and extracted three times with ether. The organic phase was washed 4 times with water, then dried with anhydrous $MgSO_4$ and concentrated via rotary evaporation. Crude product was obtained (4.1g) and used directly. Then, crude product was dissolved in THF (approx. 1 M solution) at room temperature, TMPMgCl·LiCl (13.7mL, 1 M solution) was added dropwise and the reaction mixture stirred for 1 hour. Ethyl cyanoformate (1.5 g, 14.86 mmol) was added at -40 ℃ and the reaction mixture stirred for 1 h while warming to room temperature. The reaction mixture was quenched with half concentrated aqueous NH_4Cl solution, extracted three times with Et_2O, dried ($MgSO_4$) and concentrated in vacuo. Flash column chromatographical purification on silica gel afforded compound 2 (3.1 g, 58%) as a light oil.^{1}H NMR (500 MHz, $CDCl_3$, δ): 7.25 (s, 1H), 4.45 (q, *J* = 7.1 Hz, 2H), 1.45 (t, *J* = 7.1 Hz, 3H), 1.36 (h, *J* = 7.4 Hz, 3H), 1.12 (d, *J* = 7.4 Hz, 18H).^{13}C NMR (125 MHz, $CDCl_3$, δ): 161.44, 142.57,

139.21, 139.00, 134.60, 126.20, 122.15, 77.53, 77.28, 77.02, 61.64, 18.96, 18.81, 14.57, 12.01.

Synthesis of ***Compound 2***

An oven-dried two-necked round bottom flask was charged with compound TT-Cl-COOEt (2.1 g, 5.18 mmol), compound **1** (1.1 g, 2.07 mmol), K_3PO_4 (2.2 g, 10.35 mmol), dioxane (15 mL), and H_2O (3 mL), and purged with argon for 1 h. $Pd(OAc)_2$ (93.0 mg, 0.41 mmol) and Sphos (170.0 mg, 0.41 mmol) were added subsequently under argon. The resultant mixture was then heated at 110 ℃ for 15 h. After cooling to room temperature, Then the mixture was extracted three times with dichloromethane, dried ($MgSO_4$) and concentrated in vacuo. the crude product was purified by Slica column chromatography, and a yellow oil was obtained (1.1 g, 52%). ^{1}H NMR (500 MHz, $CDCl_3$, δ): 8.13 (d, J = 8.0 Hz, 2H), 7.61 (s, 2H), 7.46 (d, J = 8.0 Hz, 2H), 7.40 (s, 2H), 4.30 (q, J = 7.1 Hz, 4H), 4.20 (d, J = 7.4 Hz, 2H), 1.40 (m, 13H), 1.31 - 1.20 (m, 14H), 1.18 (d, J = 7.4 Hz, 37H), 0.93 (t, J = 7.4 Hz, 3H), 0.84 (t, J = 7.0 Hz, 3H). ^{13}C NMR (125 MHz, $CDCl_3$, δ): 157.23, 149.63, 140.51, 135.80, 133.61, 132.37, 126.42, 121.07, 117.65, 116.18, 115.34, 114.55, 105.48, 72.01, 71.75, 71.50, 55.57, 42.40, 34.16, 25.74, 23.44, 19.02, 17.77, 13.37, 8.86, 8.72, 6.56, 5.57.

Synthesis of ***Compound 3***

To a solution of 4-hexyl-1-bromobenzene (851 mg, 3.53 mmol) in THF (25 mL) at -78 °C was added n-BuLi (1.36 mL, 3.26 mmol, 2.5 M in hexane) and the mixture was kept at -78 °C for 1 h. A solution of compound **2** (550 mg, 0.54 mmol) in THF (15 mL) was then added slowly. The mixture was stirred at room temperature overnight, then

poured into water and extracted twice with ethyl acetate. The combined organic layer was dried over $MgSO_4$. After removal of the solvent under reduced pressure, the residue was dissolved in anhydrous dichloromethane (30 mL), then several drops of $BF_3 \cdot Et_2O$ was added slowly. The resulting solution was stirred at room temperature for 1 h and then quenched with water. The organic layer was washed with water for three times and extracted with petroleum ether (3×50 mL). The combined organic phase was dried over anhydrous $MgSO_4$. Then, the crude products were purified by column chromatography on silica gel using petroleum ether/ dichloromethane (10:1, v/v) to give a yellow solid (340mg, 2 steps overall yield 41%).^{1}H NMR (500 MHz, $CDCl_3$, δ):7.92 (s, 2H), 7.40 (s, 2H), 7.36 (s, 2H), 7.24 - 7.20 (m, 9H), 7.05 (d, J = 8.1 Hz, 8H), 4.22 (m, 2H), 2.56 - 2.51 (m, 8H), 1.59 - 1.53 (m, 8H), 1.38 - 1.23 (m, 36H), 0.96 (d, J = 30.6 Hz, 7H), 0.85 (t, J = 6.7 Hz, 13H). ^{13}C NMR (125 MHz, $CDCl_3$, δ): 140.83, 139.62, 139.04, 137.99, 136.16, 136.11, 136.06, 133.94, 131.68, 130.72, 123.04, 122.88, 122.54, 116.24, 112.23, 94.24, 72.03, 71.78, 71.52, 57.33, 42.69, 34.04, 30.33, 26.46, 26.02, 25.48, 23.91, 23.33, 19.24, 17.93, 17.35, 13.38, 8.96, 8.85, 6.58, 5.82.

Synthesis of ***Compound 4 (CZTT)***

Tetrabutylammonium fluoride trihydrate (1.67 mL, 1 M in THF, 1.67 mmol) was added to a solution of the compound **3** (320 mg, 0.21 mmol) in THF (0.01M). The reaction mixture was stirred for 16 h in the absence of light. The organic layer was washed with water for three times and extracted with petroleum ether (3×50 mL). The combined organic phase was dried over anhydrous $MgSO_4$. Then, the crude products were purified by column chromatography on silica gel using petroleum ether/

dichloromethane (10:1, v/v) to give a yellow solid (240 mg, yield 94%).^{1}H NMR (500 MHz, $CDCl_3$) δ 7.92 (s, 2H), 7.36 (s, 2H), 7.31 (d, J = 5.2 Hz, 2H), 7.28 (s, 2H), 7.21 - 7.17 (m, 8H), 7.04 (d, J = 8.1 Hz, 8H), 4.22 (m, 2H), 2.55 - 2.50 (m, 8H), 1.27 (m, 37H), 0.96 (m, 7H), 0.85 (t, J = 6.8 Hz, 13H). ^{13}C NMR (125 MHz, $CDCl_3$, δ): 141.25, 139.74, 138.43, 136.26, 136.19, 136.09, 136.01, 130.55, 128.70, 123.10, 122.80, 121.12, 116.25, 115.09, 112.20, 94.23, 72.04, 71.78, 71.53, 57.27, 42.52, 34.13, 30.35, 26.46, 26.04, 25.57, 23.96, 23.41, 19.27, 17.92, 17.35, 8.96, 8.85, 5.82.

Synthesis of ***Compound 5***

To a solution of compound **4** (157 mg, 0.13 mmol) in dry 8 mL 1,2-dichloroethane ($ClCH_2CH_2Cl$) and 3 mL DMF was dropped 0.2 mL of phosphorus oxychloride ($POCl_3$) at 0 °C under the protection of nitrogen. The mixture was stirred at 0 °C for 0.5 h. After refluxing at 85 °C overnight, the mixture was poured into ice water (100 mL), neutralized with saturated sodium hydroxide solution, and then extracted with ethyl acetate twice. The combined organic layer was washed with water and brine, dried over $MgSO_4$, and evaporated under reduced pressure. The crude product was purified by silica gel using petroleum ether/dichloromethane (2:1, v/v) as eluent, yielding an orange solid (130 mg, 79.2%). ^{1}H NMR (500 MHz, $CDCl_3$, δ): 9.93 (s, 2H), 8.01 (d, *J* = 11.1 Hz, 4H), 7.49 (s, 2H), 7.20 (d, *J* = 7.0 Hz, 8H), 7.10 (d, *J* = 8.3 Hz, 8H), 4.29 (m, 2H), 2.59 - 2.54 (m, 8H), 1.32 (m, 36H), 1.01 (d, *J* = 28.3 Hz, 7H), 0.89 (t, *J* = 6.8 Hz, 14H). ^{13}C NMR (125 MHz, $CDCl_3$, δ) :183.47, 151.05, 147.29, 146.59, 144.72, 142.60, 142.25, 142.01, 141.20, 140.97, 135.73, 130.49, 129.25, 128.49, 123.30, 118.56, 101.26, 77.93, 77.68, 77.42, 63.24, 40.02, 36.22, 32.33, 31.92, 31.44, 29.81, 29.28, 25.14, 23.77,

23.22, 14.78, 11.70, 0.27.

*Synthesis of **CZTT-IC***

Compound **5** (108.0 mg, 84.58 μmol), 2-(3-oxo-2,3-dihydro-1H-inden-1-ylidene) malononitrile (91.25 mg, 507.47 μmol) and pyridine (0.1 mL) were dissolved in dry $CHCl_3$ (10mL). The mixture was deoxygenated with nitrogen for 15 min and then stirred at reflux for 7 h. After cooling to room temperature, the mixture was poured into methanol (150 mL) and filtered. The residue was purified by column chromatography on silica gel using petroleum ether/dichloromethane (1: 1, v/v) as eluent, yielding a blue solid (100 mg, 73%). ^{1}H NMR (500 MHz, $CDCl_3$, δ): 8.85 (s, 2H), 8.65 (d, *J* = 5.9 Hz, 2H), 8.13 (s, 2H), 8.00 (s, 2H), 7.91 (d, *J* = 5.6 Hz, 2H), 7.74 (d, *J* = 6.1 Hz, 4H), 7.41 (s, 2H), 7.24 (d, *J* = 1.8 Hz, 8H), 7.12 (d, *J* = 8.0 Hz, 8H), 4.23 - 4.07 (m, 2H), 2.57 - 2.52 (m, 9H), 1.60 - 1.55 (m, 12H), 1.38 - 1.23 (m, 36H), 0.88 (t, *J* = 13.5, 7.0 Hz, 19H). ^{13}C NMR (125 MHz, $CDCl_3$, δ): 188.39, 160.36, 154.44, 147.85, 147.58, 147.12, 143.57, 142.47, 142.09, 140.39, 140.16, 139.48, 138.44, 137.24, 137.02, 135.36, 135.28, 134.64, 129.02, 128.21, 125.41, 123.91, 123.64, 122.39, 118.38, 114.96, 114.86, 101.23, 77.53, 77.48, 77.28, 77.02, 69.23, 63.03, 48.04, 39.49, 35.85, 31.94, 31.53, 30.98, 29.95, 29.47, 28.82, 24.68, 23.30, 22.83, 14.35, 14.32, 11.20, 0.25.

MALDI-TOF MS: m/z= 1627.8079. [M], calcd. for $C_{108}H_{101}N_5O_2S_4$: 1627.6838.

*Synthesis of **CZTT-4F***

Compound **5** (108.0 mg, 84.58 μmol), 2-(5,6-difluoro-3-oxo-2,3-dihydro-1H-inden-1-ylidene) malononitrile (116.7 mg, 507.47 μmol) and pyridine (0.1 mL) were dissolved in dry $CHCl_3$ (10mL). The mixture was deoxygenated with nitrogen for 15 min and then

stirred at reflux for 7 h. After cooling to room temperature, the mixture was poured into methanol (150 mL) and filtered. The residue was purified by column chromatography on silica gel using petroleum ether/dichloromethane (1: 1, v/v) as eluent, yielding a blue solid (100 mg, 72.5%). ^{1}H NMR (500 MHz, $CDCl_3$, δ): 8.85 (s, 2H), 8.52 (d, *J* = 3.3 Hz, 2H), 8.19 (s, 2H), 8.01 (s, 2H), 7.68 (t, *J* = 7.5 Hz, 2H), 7.42 (s, 2H), 7.24 (d, *J* = 7.4 Hz, 8H), 7.12 (d, *J* = 8.2 Hz, 8H), 4.15 (m, 2H), 2.60 - 2.49 (m, 8H), 1.61 - 1.49 (m, 11H), 1.49 - 1.20 (m, 35H), 1.01 - 0.78 (m, 19H). ^{13}C NMR (125 MHz, $CDCl_3$, δ): 185.64, 158.12, 155.39, 155.28, 154.94, 153.30, 148.15, 147.35, 147.33, 146.86, 143.45, 142.11, 142.08, 141.85, 139.84, 138.98, 138.26, 137.31, 136.44, 134.87, 128.63, 127.75, 123.49, 121.19, 118.04, 114.88, 114.70, 114.11, 112.53, 101.11, 77.13, 76.88, 76.62, 69.32, 62.60, 35.45, 31.55, 31.10, 30.64, 29.06, 28.47, 24.31, 22.95, 22.43, 13.98, 13.92, 10.86. MALDI-TOF MS: m/z= 1699.6270. [M], calcd. for $C_{108}H_{97}F_4N_5O_2S_4$: 1699.6461.

2. NMR and Mass Spectra

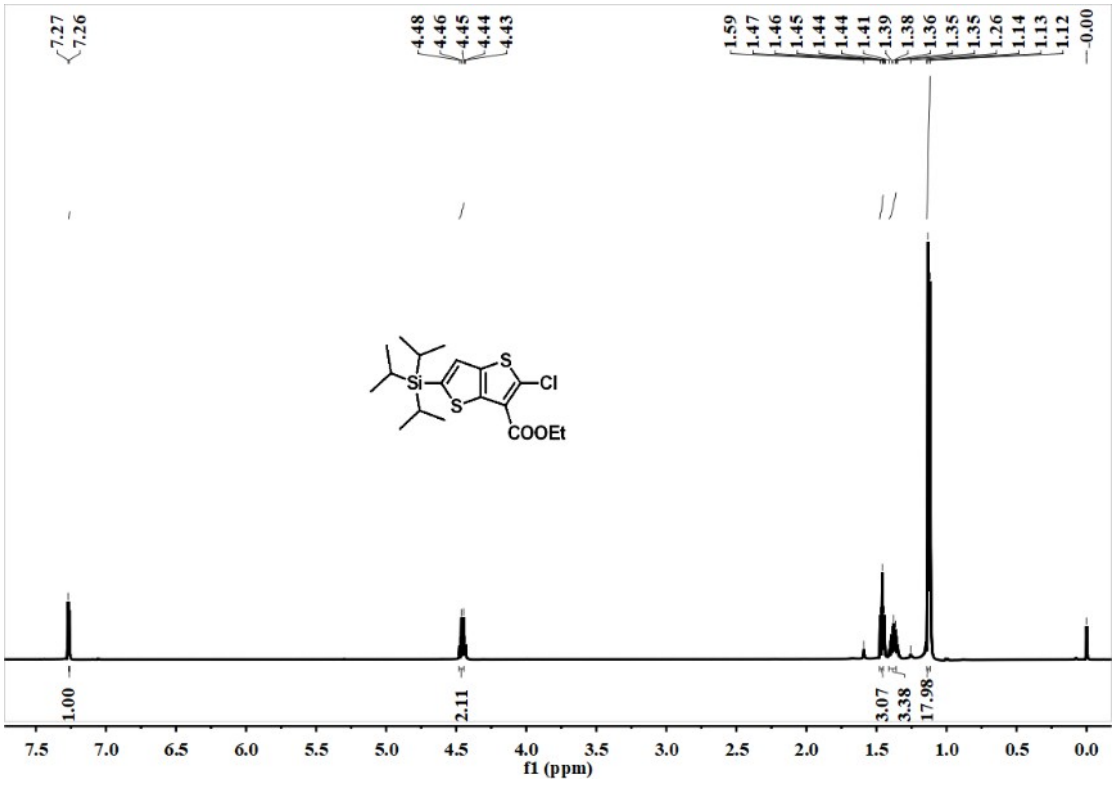

Fig. S1. ^{1}H NMR spectrum of **TT-Cl-COOEt**.

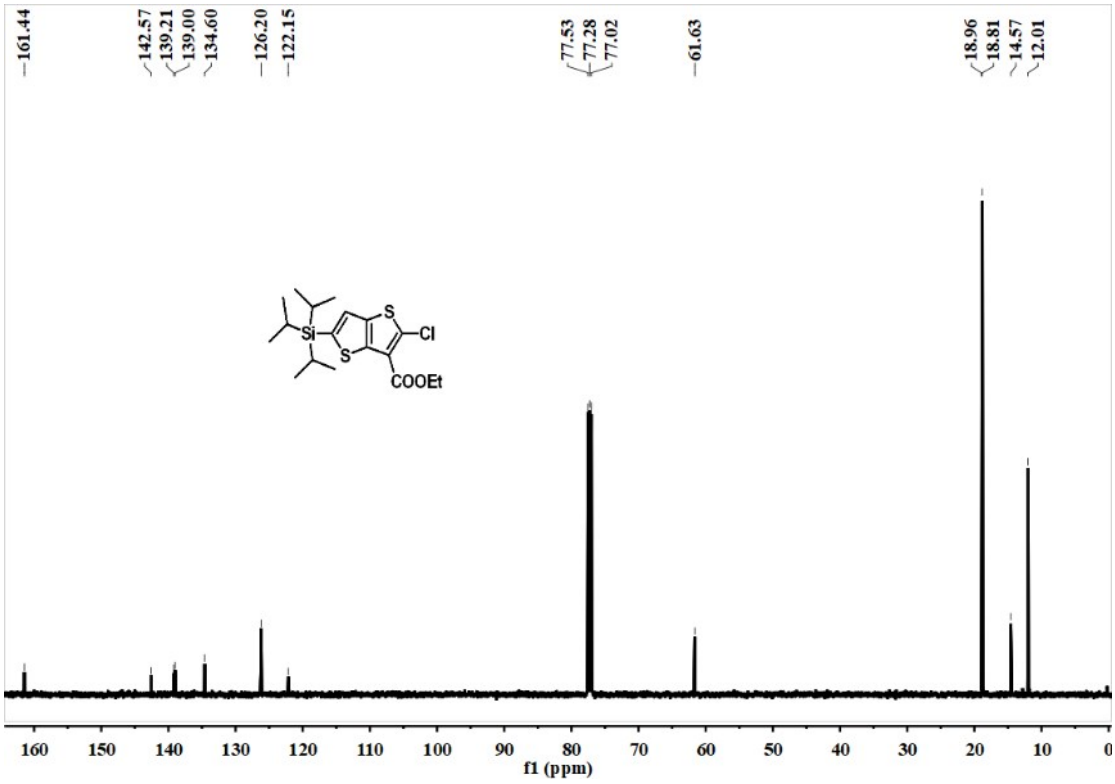

Fig. S2. ^{13}C NMR spectrum of **TT-Cl-COOEt**.

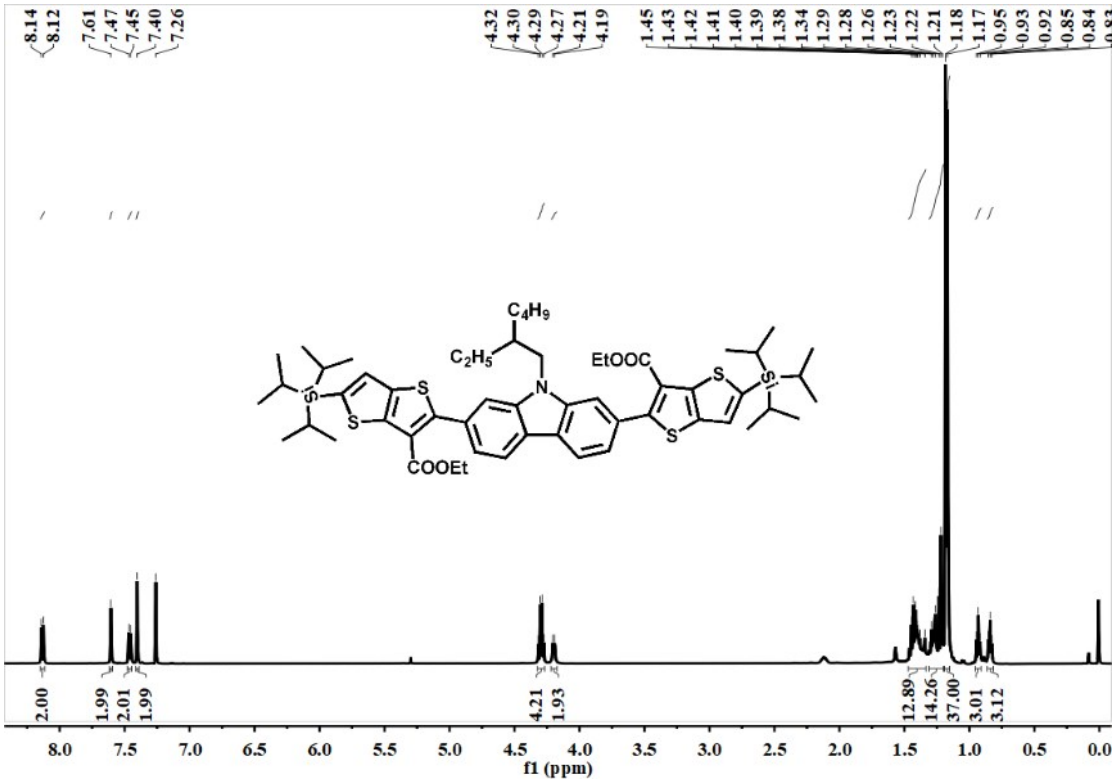

Fig. S3. ^{1}H NMR spectrum of **compound 2**.

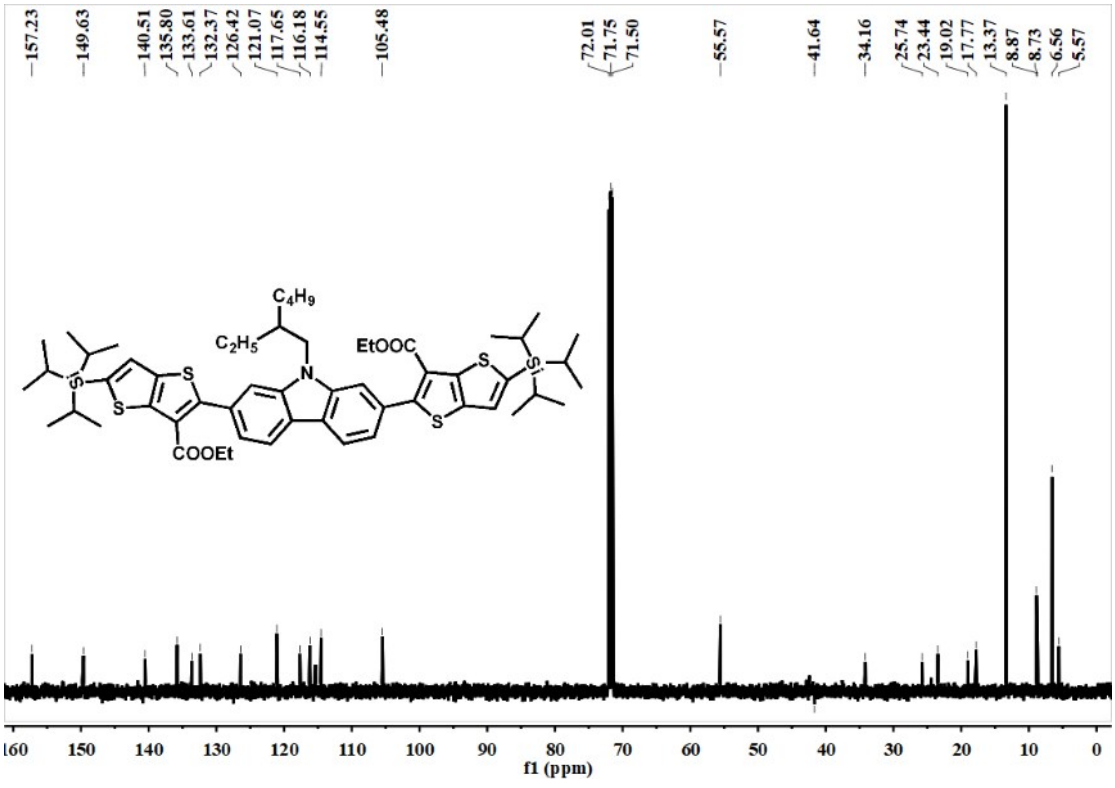

Fig. S4. ^{13}C NMR spectrum of **compound 2**.

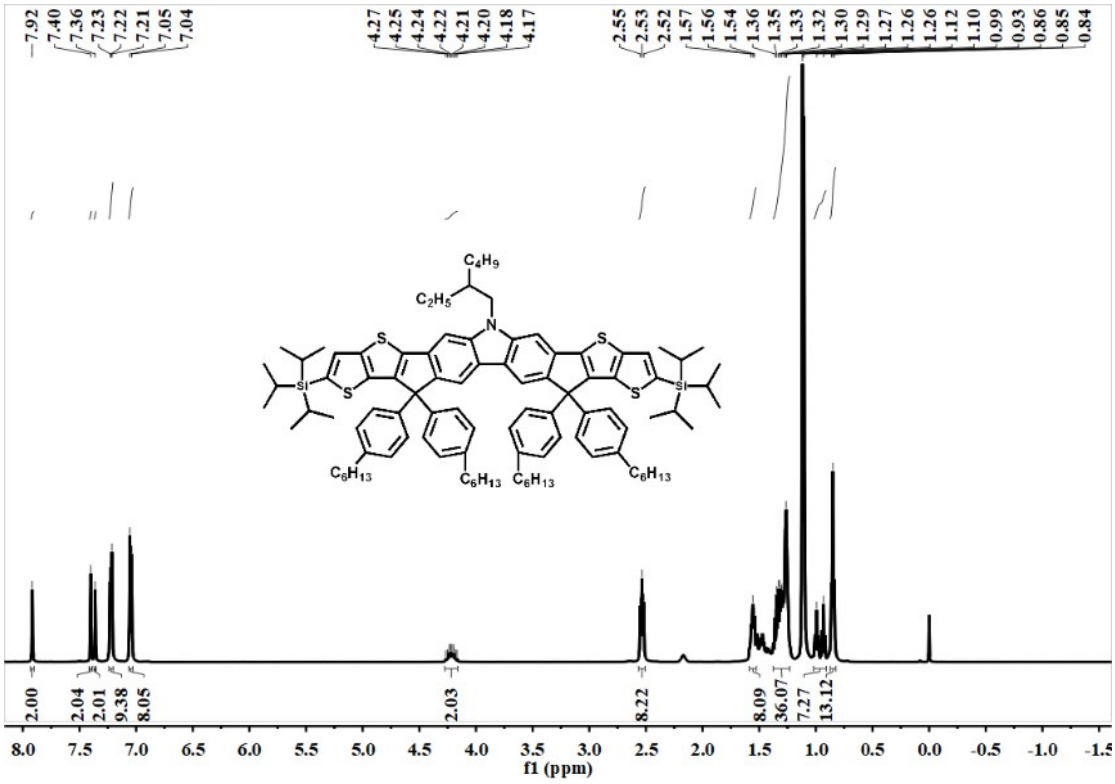

Fig. S5. ^{1}H NMR spectrum of **compound 3**.

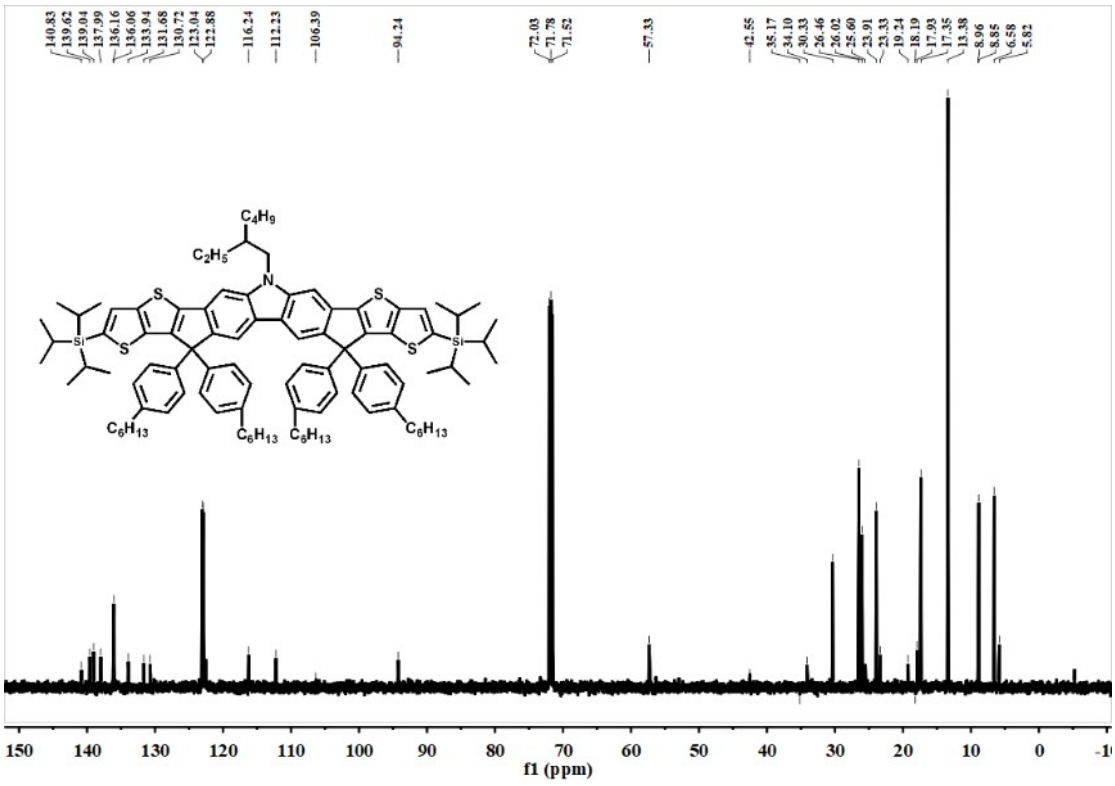

Fig. S6. ^{13}C NMR spectrum of **compound 3**.

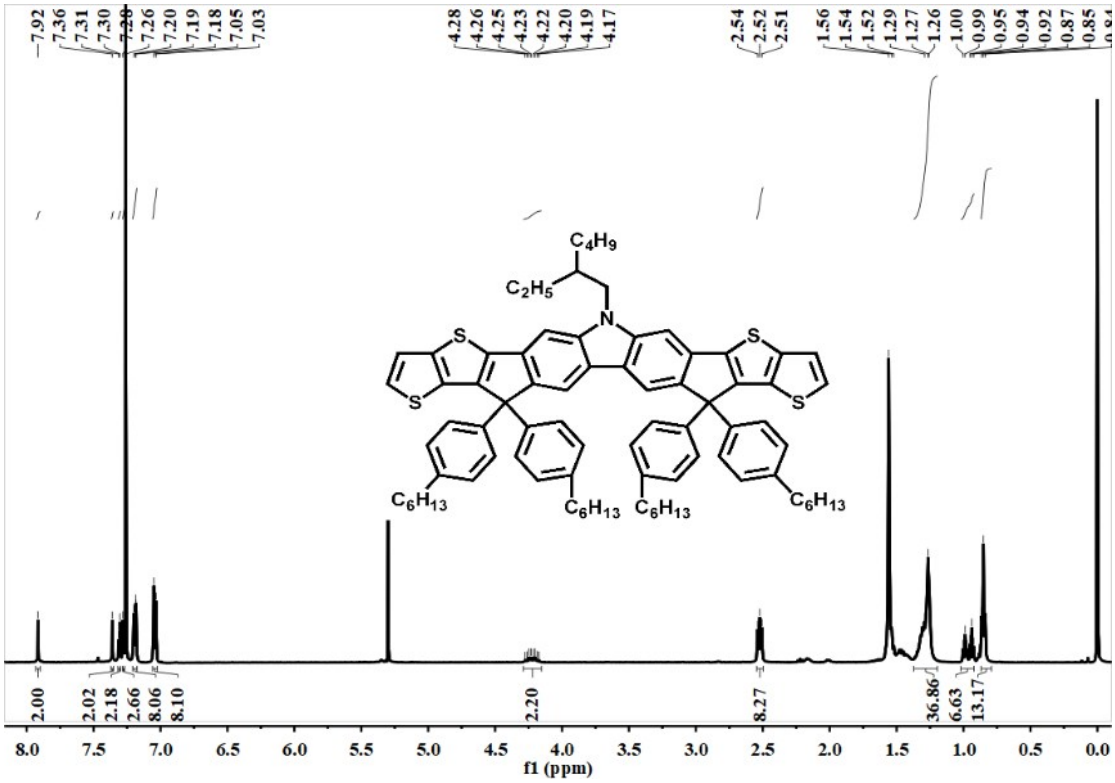

Fig. S7. ^{1}H NMR spectrum of **compound 4 (CZTT)**.

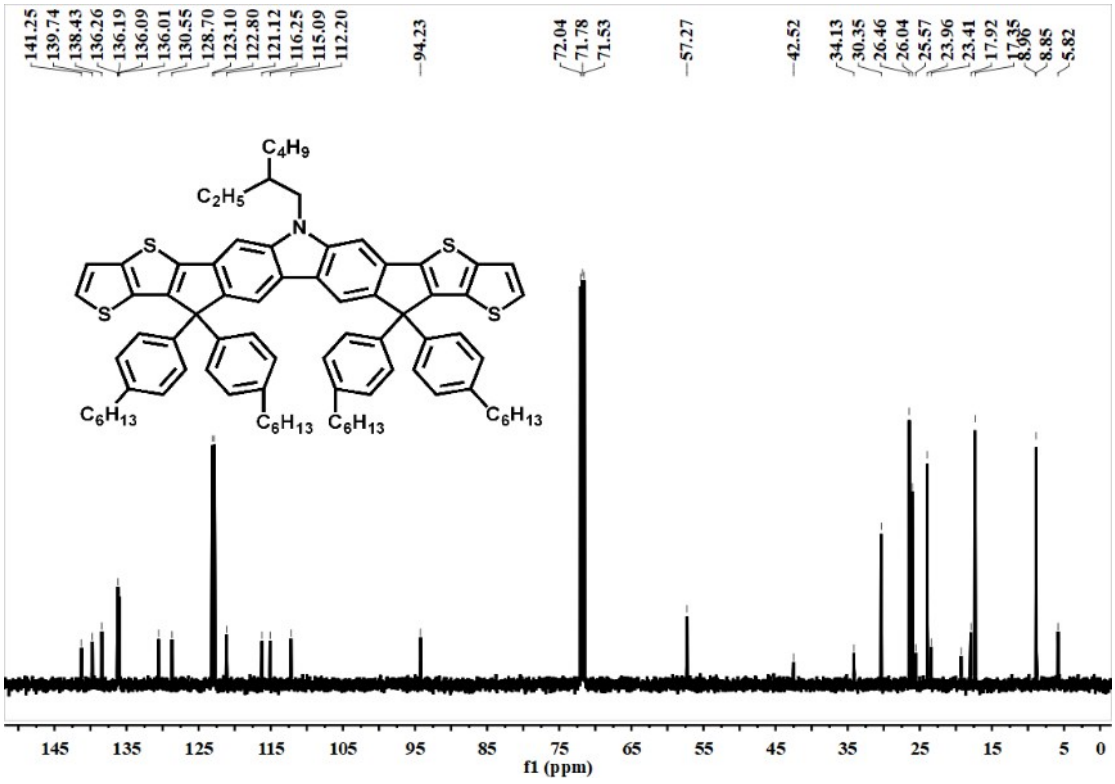

Fig. S8. ^{13}C NMR spectrum of **compound 4 (CZTT)**.

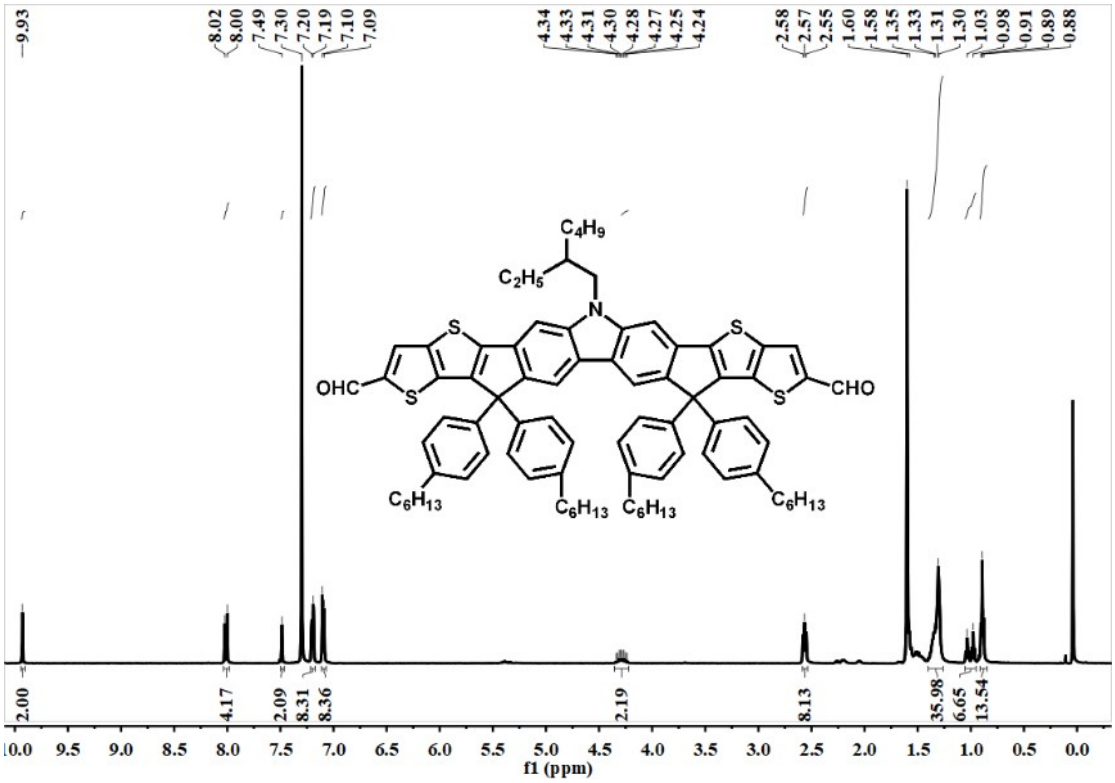

Fig. S9. ^{1}H NMR spectrum of **compound 5**.

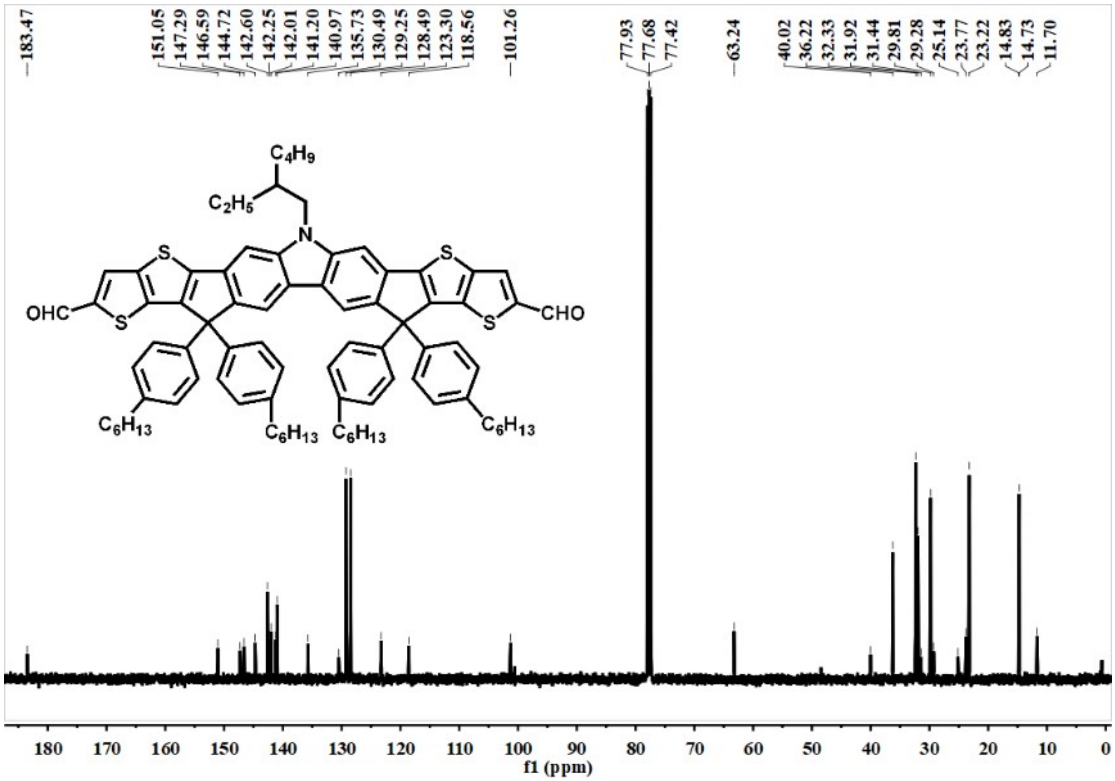

Fig. S10. ^{13}C NMR spectrum of **compound 5**.

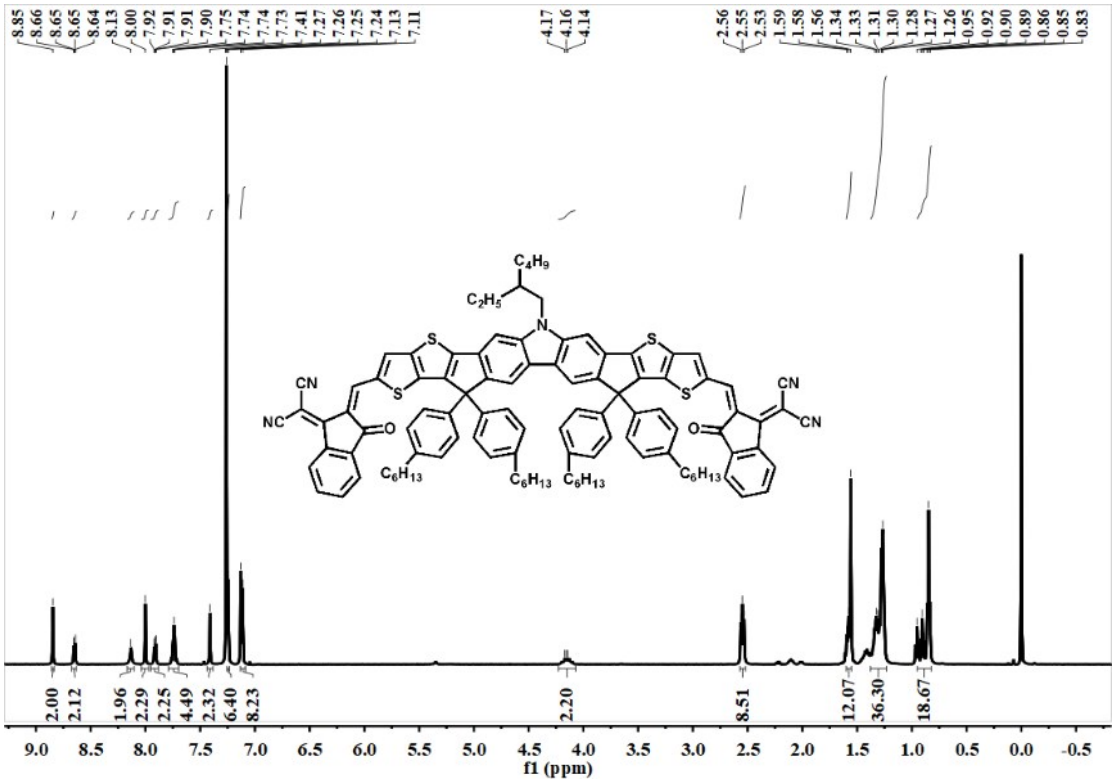

Fig. S11. ^{1}H NMR spectrum of **CZTT-IC**.

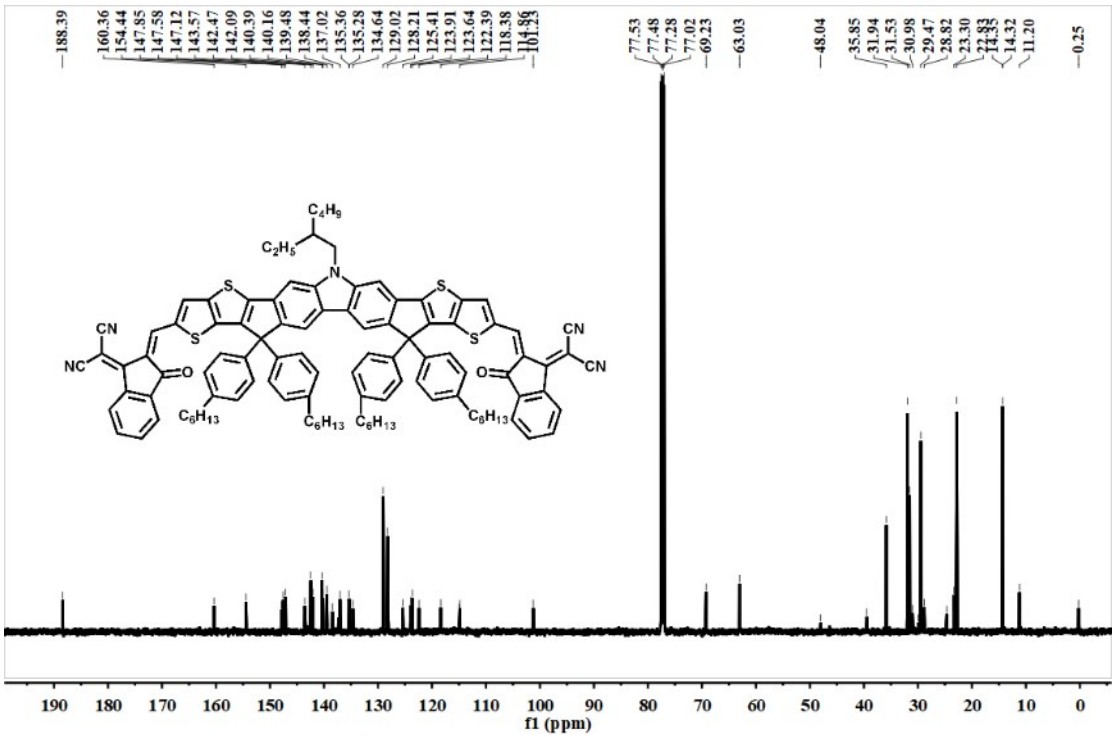

Fig. S12. ^{13}C NMR spectrum of **CZTT-IC**.

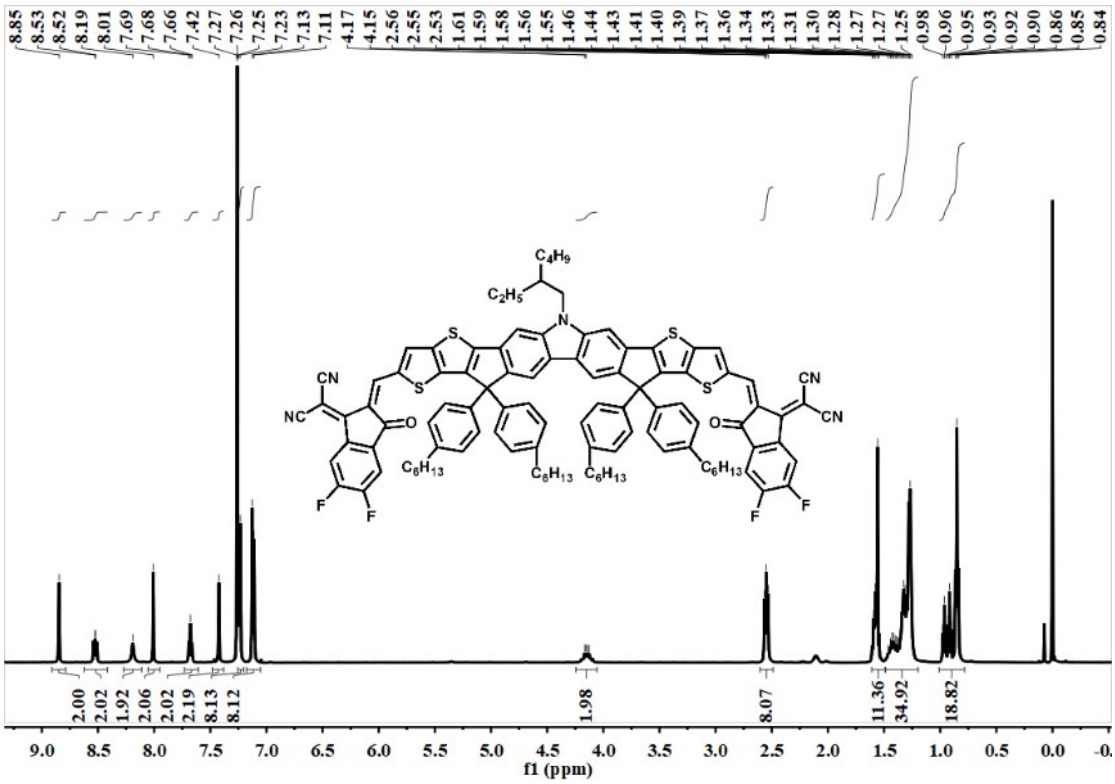

Fig. S13. ^{1}H NMR spectrum of **CZTT-4F**.

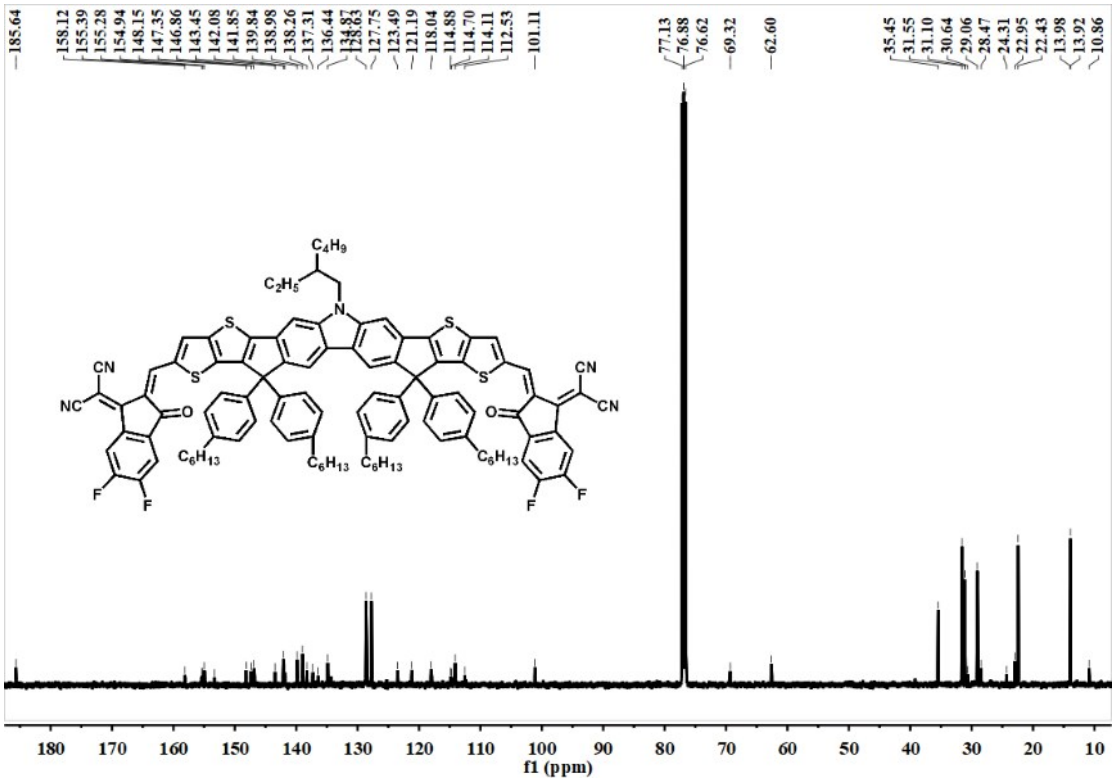

Fig. S14. ^{13}C NMR spectrum of **CZTT-4F**.

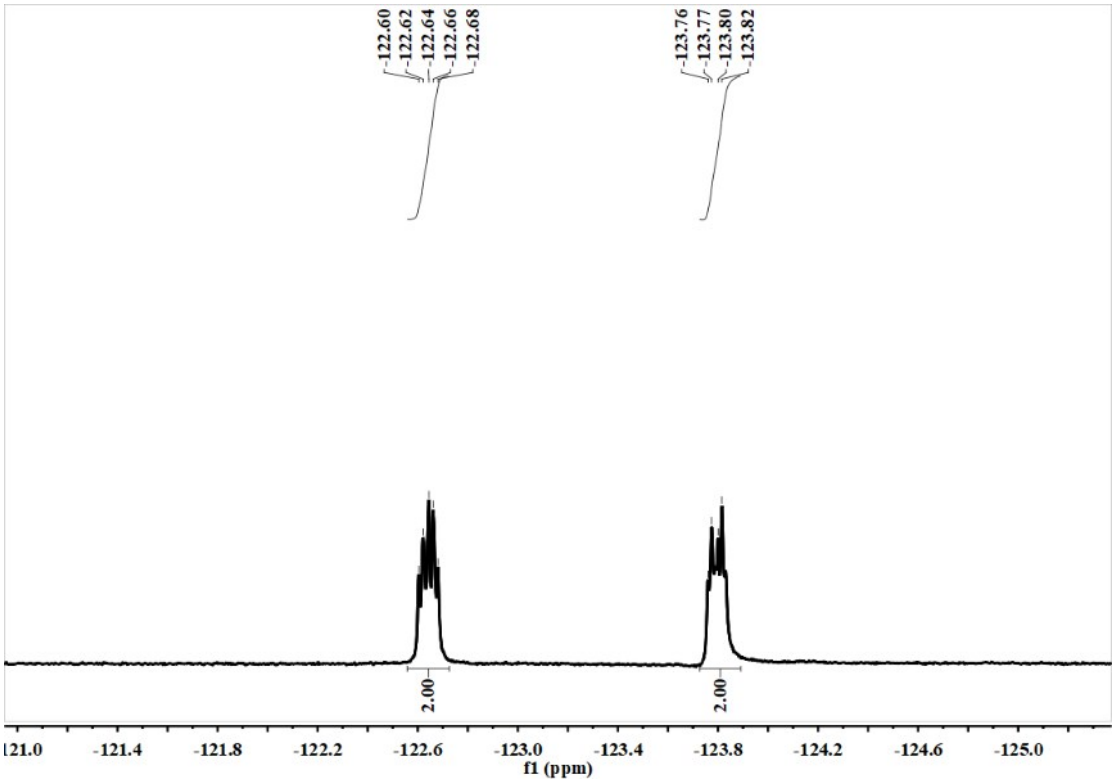

Fig. S15. ^{19}F NMR spectrum of **CZTT-4F**.

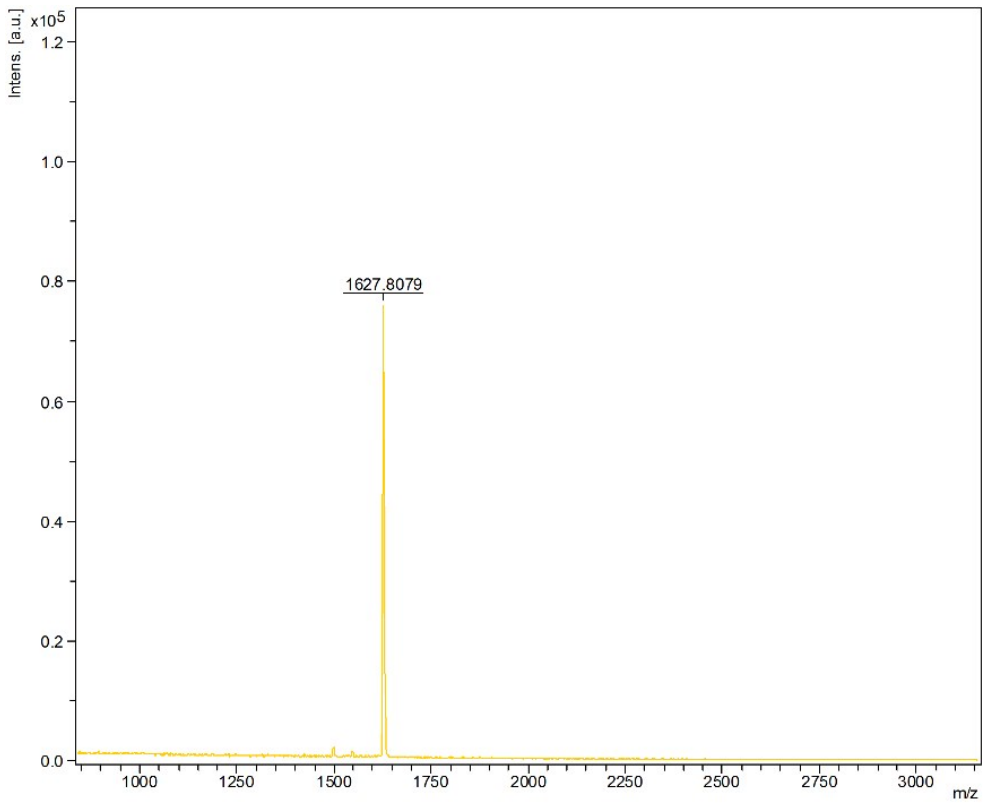

Fig. S16. The MALDI-TOF MS plots of **CZTT-IC**.

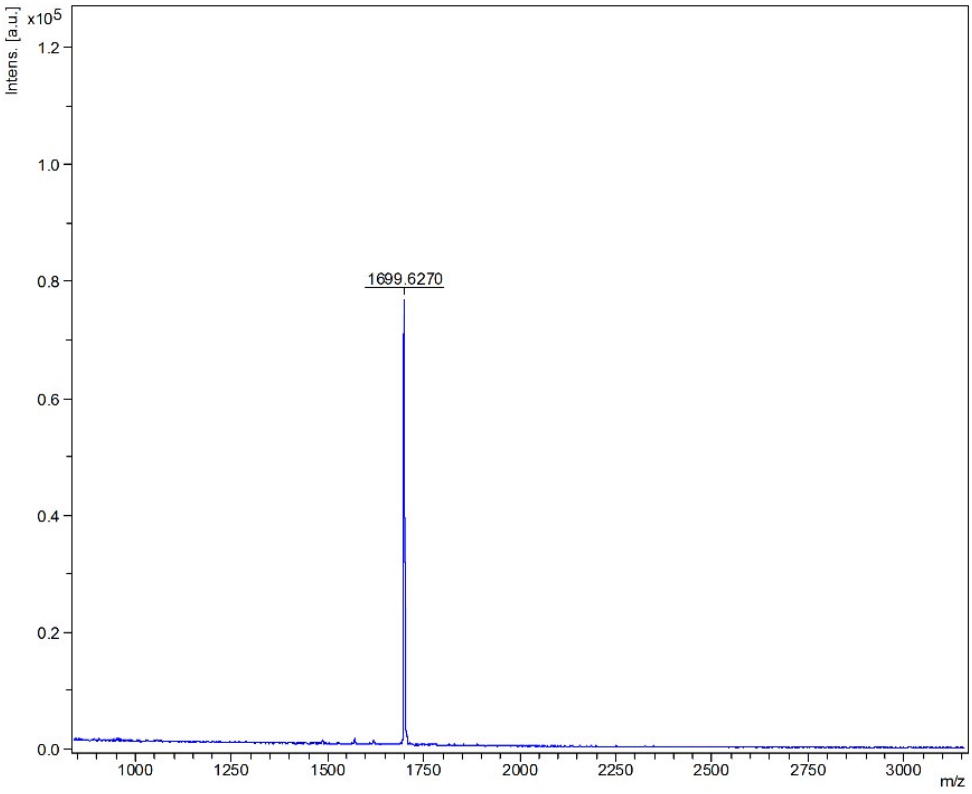

Fig. S17. The MALDI-TOF MS plots of **CZTT-4F**.

3. TG Analysis, UV-vis Absorption and CV measurement

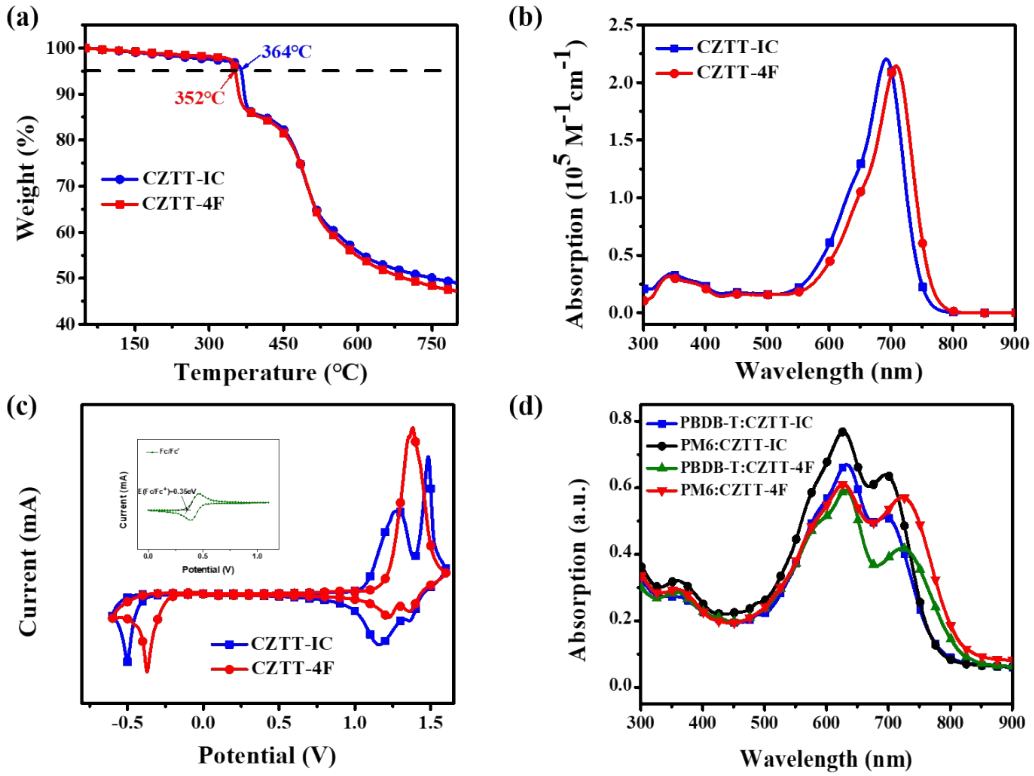

Fig. S18. (a) TGA traces. (b) Absorption spectra of two acceptors in chloroform solution (10^{-5} M). (c) Cyclic voltammograms for CZTT-IC and CZTT-4F in CH_3CN/0.1 M *n*-Bu_4NPF_6 at 50 mV s^{-1}. (d) BHJ Absorption spectra of optimized blend films.

4. Theoretical Calculation

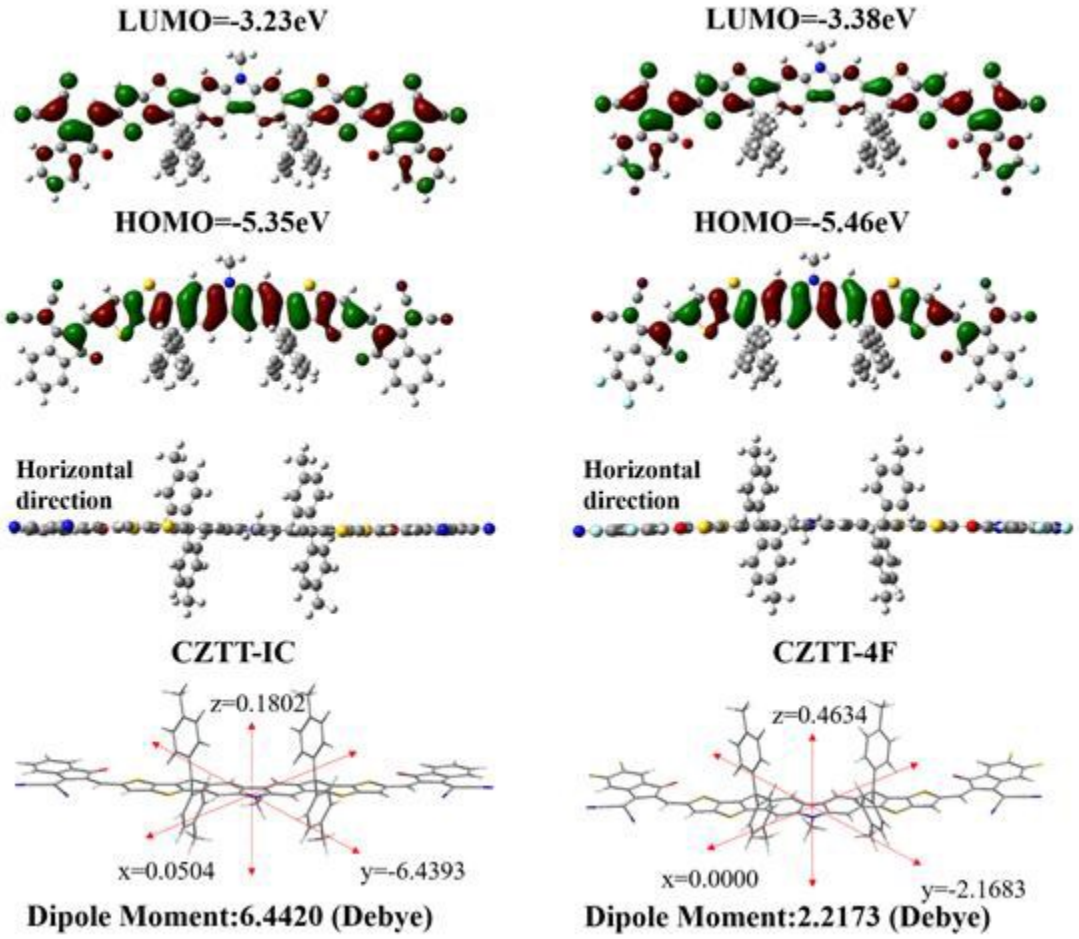

Fig. S19. Simulated frontier molecular orbits, molecular conformations and calculated molecular dipole moments of CZTT-IC and CZTT-4F.

5. SCLC Mobility Measurements and charge extraction

Table S1. Hole and electron mobilities of the blend films.

Blend Film	μ_h [cm^2 V^{-1} s^{-1}]	μ_e [cm^2 V^{-1} s^{-1}]	μ_e/μ_h
PBDB-T:CZTT-IC	6.48×10^{-4}	8.55×10^{-4}	1.32
PM6:CZTT-IC	1.12×10^{-4}	2.68×10^{-4}	2.39
PBDB-T:CZTT-4F	4.34×10^{-4}	6.67×10^{-4}	1.54
PM6:CZTT-4F	1.68×10^{-3}	1.88×10^{-3}	1.12

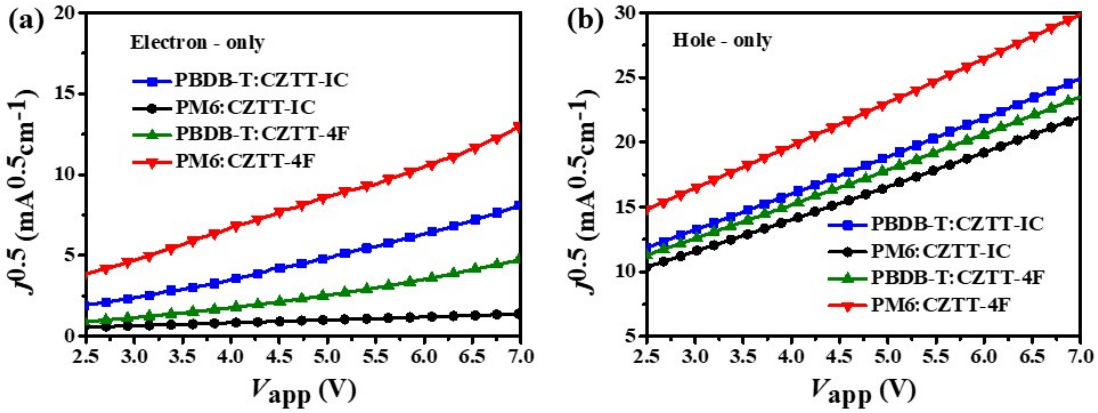

Fig. S20. $J^{0.5}$–V characteristics were acquired from (a) electron-only and (b) hole-only devices with blend films.

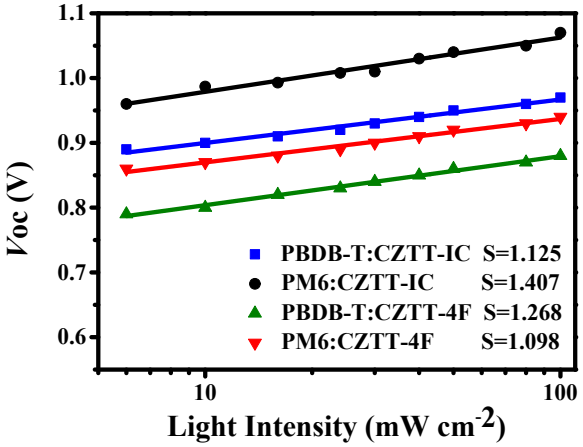

Fig. S21. Dependence of the open circuit voltage (V_{OC}) on the excitation light intensity.

6. Optimization of binary OSCs

Table S2. The optimized photovoltaic parameters of devices based on PBDB-T:CZTT-IC with different D/A ratios.

D/A	V_{OC} (V)	J_{SC} (mA cm^{-2})	FF (%)	PCE [a] (%)
1:0.8	0.99 (0.99±0.01)	16.08 (15.84±0.26)	49.89 (50.19±0.59)	7.94 (7.85±0.09)
1:1	**0.98** **(0.99±0.01)**	**16.76** **(16.53±0.33)**	**50.39** **(50.00±0.41)**	**8.28** **(8.13±0.18)**
1:1.25	0.98 (0.98±0.01)	14.76 (14.80±0.14)	44.17 (43.86±0.39)	6.39 (6.27±0.18)

a) The average values were obtained from 12 devices.

Table S3. The optimized photovoltaic parameters of devices based on PBDB-T:CZTT-IC=1:1 at different thermal annealing temperature (TAT) with 0.5% DIO additives.

TAT(℃)	V_{OC}(V)	J_{SC}(mA cm^{-2})	FF(%)	PCE [a](%)
-	0.99 (0.99±0.00)	17.10 (16.74±0.38)	50.85 (50.43±0.62)	8.61 (8.58±0.03)
100	0.98 (0.99±0.01)	17.06 (16.60±0.47)	57.04 (56.37±0.77)	9.54 (9.42±0.12)
120	**0.97** **(0.97±0.01)**	**17.26** **(17.15±0.13)**	**58.97** **(58.29±0.66)**	**9.87** **(9.83±0.15)**
135	0.97 (0.97±0.00)	16.53 (16.43±0.15)	57.01 (56.68±0.43)	9.14 (9.11±0.07)

a) The average values were obtained from over 12 devices.

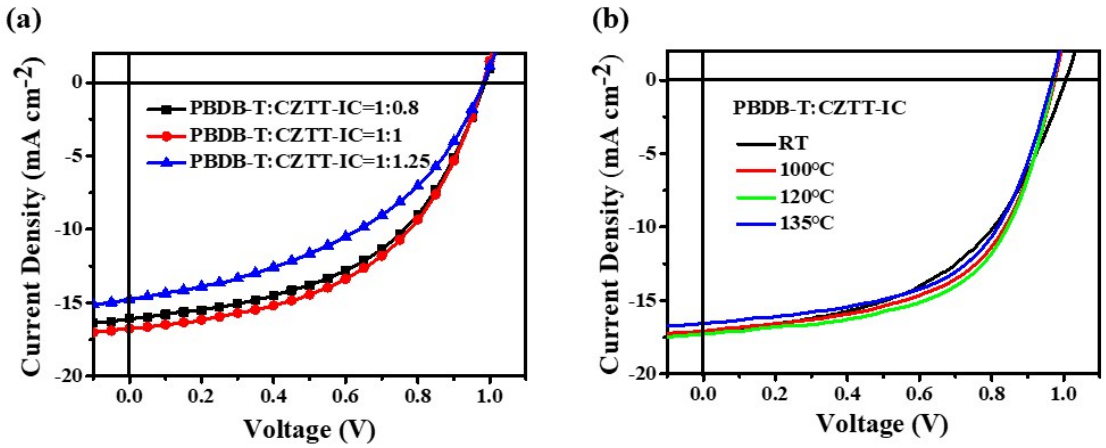

Fig. S22. a) *J*–*V* curves of PBDB-T:CZTT-IC based devices with different D/A ratios. b) *J*-*V* curves of devices based on PBDB-T:CZTT-IC=1:1 films with different thermal annealing temperature for 10 min with 0.5% DIO additives.

Table S4. The optimized photovoltaic parameters of devices based on PM6:CZTT-IC with different D/A ratios.

D/A	V_{OC} (V)	J_{SC} (mA cm^{-2})	FF (%)	PCE [a] (%)
1:0.8	1.08 (1.09±0.01)	11.79 (11.63±0.26)	46.67 (46.02±0.65)	5.94 (5.81±0.09)
1:1	**1.08** **(1.08±0.00)**	**12.06** **(11.74±0.18)**	**49.08** **(48.54±0.55)**	**6.39** **(6.28±0.07)**
1:1.25	1.08 (1.09±0.01)	12.16 (12.01±0.19)	46.55 (46.06±0.59)	6.11 (5.98±0.16)

a) The average values were obtained from 12 devices.

Table S5. The optimized photovoltaic parameters of devices based on PM6:CZTT-IC =1:1 at different thermal annealing temperature with 0.5% DIO additives.

TAT (℃)	V_{OC} (V)	J_{SC} (mA cm^{-2})	FF (%)	PCE [a] (%)
-	1.07 (1.06±0.01)	11.96 (11.85±0.24)	48.02 (47.39±0.69)	6.15 (6.13±0.12)
100	**1.07** **(1.07±0.00)**	**12.83** **(12.65±0.33)**	**51.16** **(50.52±0.87)**	**7.02** **(6.98±0.08)**
120	1.05 (1.06±0.01)	12.71 (12.47±0.34)	48.68 (47.64±0.94)	6.84 (6.46±0.27)

a) The average values were obtained from over 12 devices.

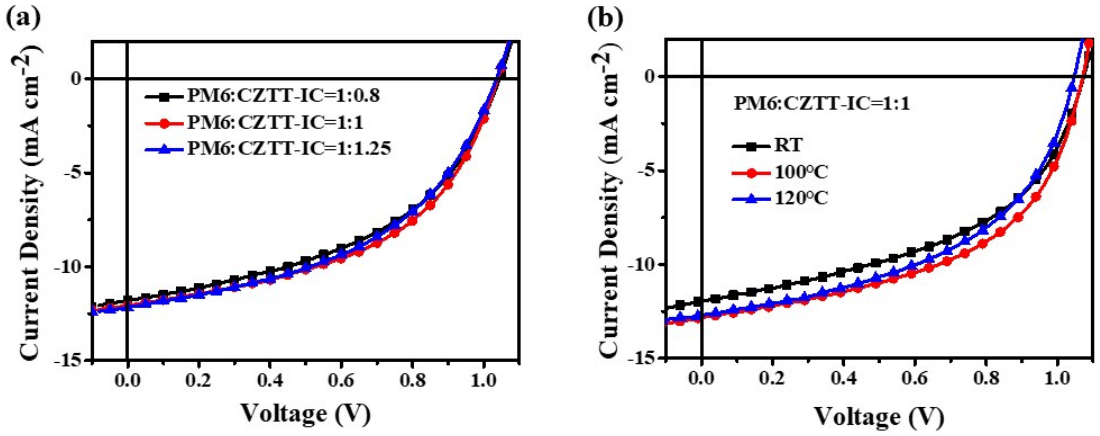

Fig. S23. a) *J*–*V* curves of PM6:CZTT-IC based devices with different D/A ratios. b) *J*-*V* curves of devices based on PM6:CZTT-IC=1:1 films with different thermal annealing temperature for 10 min with 0.5% DIO additives.

Table S6. The optimized photovoltaic parameters of devices based on PBDB-T:CZTT-4F with different D/A ratios.

D/A	V_{OC} (V)	J_{SC} (mA cm^{-2})	FF (%)	PCE [a] (%)
1:0.8	**0.88 (0.89±0.01)**	**18.30 (18.18±0.18)**	**57.94 (57.47±0.43)**	**9.33 (9.15±0.18)**
1:1	0.85 (0.84±0.01)	18.60 (18.28±0.21)	55.12 (54.45±0.56)	8.71 (8.53±0.19)
1:1.25	0.86 (0.85±0.01)	18.17 (17.98±0.26)	56.35 (55.81±0.49)	8.81 (8.72±0.12)

a) The average values were obtained from 12 devices.

Table S7. The optimized photovoltaic parameters of devices based on PBDB-T:CZTT-4F =1:0.8 at different thermal annealing temperature with 0.5% DIO additives.

TAT (℃)	V_{OC} (V)	J_{SC} (mA cm^{-2})	FF (%)	PCE [a] (%)
-	**0.88 (0.89±0.01)**	**19.06 (18.78±0.37)**	**58.47 (58.13±0.56)**	**9.81 (9.77±0.12)**
100	0.87 (0.88±0.01)	18.10 (17.69±0.46)	56.88 (56.17±0.73)	8.95 (8.71±0.28)
120	0.88 (0.88±0.00)	16.45 (16.07±0.36)	55.26 (54.62±0.61)	8.00 (7.95±0.06)

a) The average values were obtained from over 12 devices.

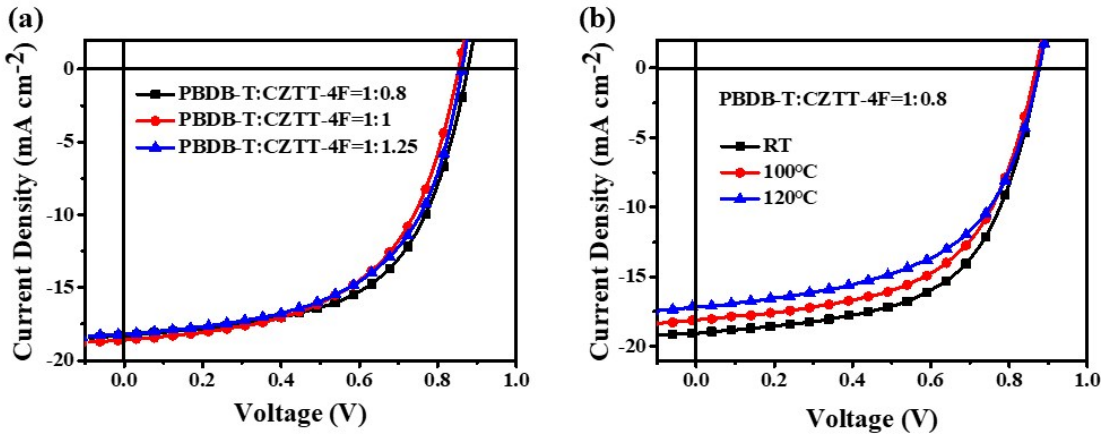

Fig. S24. a) *J*–*V* curves of PBDB-T:CZTT-4F based devices with different D/A ratios. b) *J*-*V* curves of devices based on PBDB-T:CZTT-4F=1:0.8 films with different thermal annealing temperature for 10 min with 0.5% DIO additives.

Table S8. The optimized photovoltaic parameters of devices based on PM6:CZTT-4F with different D/A ratios.

D/A	V_{OC} (V)	J_{SC} (mA cm^{-2})	FF (%)	PCE [a)] (%)
1:0.8	0.98 (0.98±0.01)	17.31 (17.18±0.24)	54.45 (53.72±0.66)	9.24 (9.06±0.16)
1:1	0.97 (0.97±0.01)	17.78 (17.46±0.43)	58.97 (58.36±0.64)	10.17 (10.00±0.15)
1:1.25	**0.96** **(0.97±0.01)**	**19.01** **(18.66±0.42)**	**59.37** **(58.73±0.58)**	**10.83** **(10.64±0.15)**

a) The average values were obtained from 12 devices.

Table S9. The optimized photovoltaic parameters of devices based on PM6:CZTT-4F =1:1.25 at different thermal annealing temperature with 0.5% DIO additives.

TAT (℃)	V_{OC} (V)	J_{SC} (mA cm^{-2})	FF (%)	PCE [a] (%)
-	0.96 (0.97±0.01)	18.43 (18.31±0.23)	61.46 (60.82±0.69)	10.86 (10.67±0.21)
100	0.96 (0.96±0.01)	18.73 (18.48±0.37)	62.87 (62.19±0.58)	11.30 (11.21±0.14)
120	0.94 (0.95±0.01)	19.11 (18.64±0.42)	64.27 (63.72±0.56)	11.55 (11.44±0.09)
135	**0.94 (0.95±0.01)**	**19.73 (19.86±0.11)**	**65.06 (64.98±0.42)**	**12.07 (11.95±0.05)**
150	0.94 (0.93±0.01)	19.12 (18.68±0.46)	59.94 (59.23±0.72)	10.77 (10.63±0.24)

a) The average values were obtained from over 12 devices.

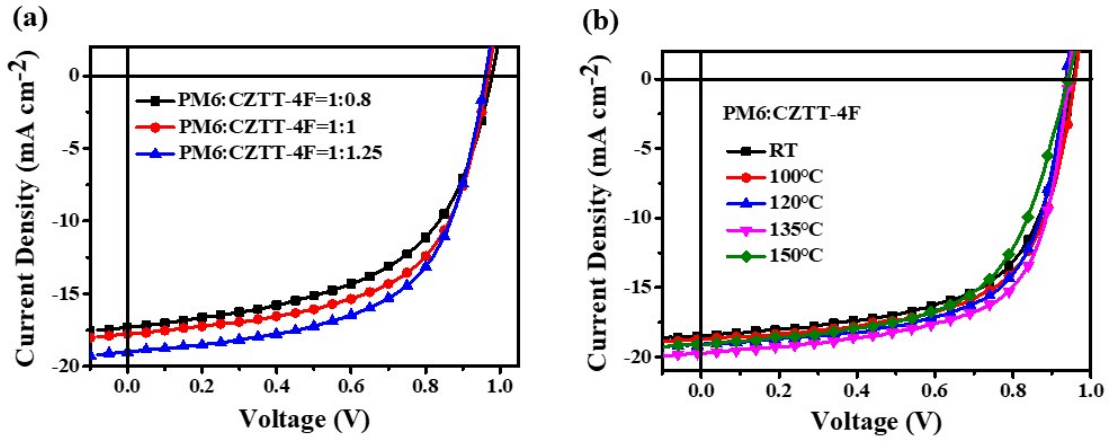

Fig. S25. a) *J*–*V* curves of PM6:CZTT-4F based devices with different D/A ratios. b) *J*-*V* curves of devices based on PM6:CZTT-4F=1:1.25 films with different thermal annealing temperature for 10 min with 0.5% DIO additives.

7. Statistical data for optimized device and summary of carbazole-based NFAs for OSCs

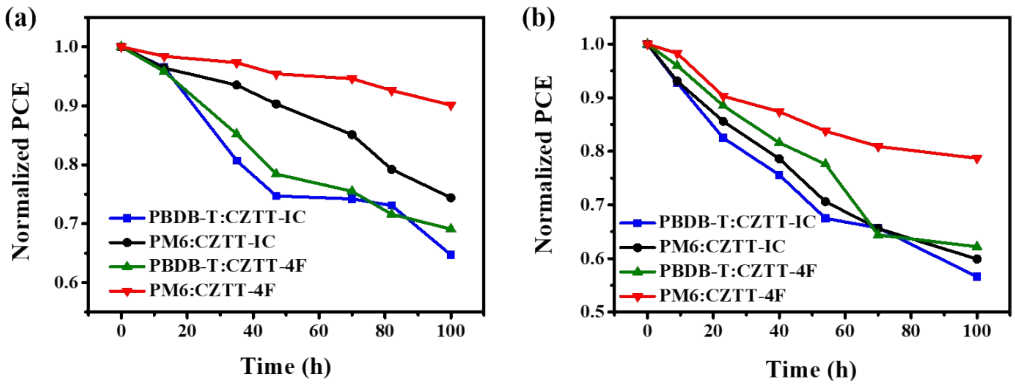

Fig. S26. Stability data of normalized PCE (a) with different annealing time at 85 ℃ (nitrogen atmosphere) and (b) with different light aging time (nitrogen atmosphere).

Table S10. Summary of A-D-A type non-fullerene based OSCs in the literature.

BHJ layer	Annealing time (h)	Annealing Temperature (℃)	PCE (%)	Initially PCE (%)	Ref.
PBDB-T:ITIC	250	100	10.8(96.3%)[a)]	11.21	1
PTZ1:IDIC	10	100	- (81.0%)[a)]	11.5	2
PBDB-T:DF-PCPC	12	150	- (86.2%)[a)]	10.14	3
PBDB-T:DF-PCPC	12	130	- (85.5%)[a)]	10.14	3
PffBT4T-2OD: EH-IDTBR	160	85	- (84%)[a)]	9.5	4
DR3TBDTC: PBN-11	168	180	- (89%)[a)]	8.01	5
PTB7Th:PBDB-T:O-IDTBR	168	85	9.37(80.9%)[a)]	11.58	6
p-DTS(FBTTh$_2$)$_2$: NCBA:PC$_{71}$BM	100	90	- (87.2%)[a)]	9.1	7
J71:ITIC: O-PYPDI	72	80	- (82%)[a)]	10.96	8
BDT(TVTSR)$_2$: IDIC	96	80	- (82%)[a)]	11.10	9

p-DTS(FBTTh$_2$)$_2$:P(NDI2OD-T$_2$)	20	180	2.03(67.2%)[a)]	3.02	10
PBDB-TF/HF-PCIC/PC$_{71}$BM	12	130	9.24 (80%)[a)]	11.55	11
PBDB-TF:HC-PCIC:PC$_{71}$BM	12	130	9.89 (80%)[a)]	12.36	11
PBTIBDTT:ITIC	96	150	7.50(84.4%)[a)]	8.89	12
PBTIBDTT:*o*F-ITIC	96	150	6.14(68.1%)[a)]	9.01	12
PBTIBDTT:*m*F-ITIC	96	150	8.90(93.7%)[a)]	9.50	12
PBDB-T:CZTT-IC	**100**	**85**	**6.65 (67.4%)[a)]**	**9.87**	**This work**
PM6:CZTT-IC	**100**	**85**	**5.22 (74.4%)[a)]**	**7.02**	**This work**
PBDB-T:CZTT-4F	**100**	**85**	**6.78 (69.1%)[a)]**	**9.81**	**This work**
PM6:CZTT-4F	**100**	**85**	**10.87 (90.1%)[a)]**	**12.07**	**This work**

a) The value in parentheses is relative to the initial PCE.

Table S11. The statistical data for optimized device based on PBDB-T:CZTT-IC, PM6:CZTT-IC, PBDB-T:CZTT-4F and PM6:CZTT-4F with different annealing time at 85℃ in glove box, under AM 1.5G solar spectrum.

Active Layer	Annealing Time	V_{OC} (V)	J_{SC} (mA cm^{-2})	FF (%)	PCE (%)
PBDB-T: CZTT-IC	0h	0.97	17.26	58.97	9.87
	13h	0.97	16.82	58.26	9.52 (96.5%)[a)]
	35h	0.92	15.26	56.77	7.97 (80.7%)[a)]
	47h	0.91	14.89	54.39	7.37 (74.7%)[a)]
	70h	0.91	14.92	53.91	7.32 (74.2%)[a)]
	82h	0.91	14.75	53.72	7.21 (73.1%)[a)]
	100h	0.91	14.12	51.75	6.65 (67.4%)[a)]
PM6: CZTT-IC	0h	1.07	12.83	51.16	7.02
	13h	1.06	12.66	50.45	6.77 (96.4%)[a)]
	35h	1.06	12.15	50.93	6.56 (93.5%)[a)]
	47h	1.06	12.06	49.59	6.34 (90.3%)[a)]
	70h	1.05	11.56	49.25	5.97 (85.1%)[a)]
	82h	1.05	11.36	46.61	5.56 (79.2%)[a)]
	100h	1.05	10.93	45.48	5.22 (74.4%)[a)]
PBDB-T: CZTT-4F	0h	0.88	19.06	58.47	9.81
	13h	0.88	18.67	57.21	9.40 (95.8%)[a)]
	35h	0.87	17.95	53.53	8.36 (85.2%)[a)]
	47h	0.86	16.84	53.10	7.69 (78.4%)[a)]
	70h	0.86	16.68	51.64	7.41 (75.5%)[a)]
	82h	0.85	16.36	50.48	7.02 (71.6%)[a)]
	100h	0.84	16.00	50.44	6.78 (69.1%)[a)]
PM6: CZTT-4F	0h	0.94	19.73	65.06	12.07
	13h	0.94	19.65	64.32	11.88 (98.4%)[a)]
	35h	0.94	19.47	64.15	11.74 (97.3%)[a)]
	47h	0.94	19.26	63.58	11.51 (95.4%)[a)]
	70h	0.94	19.21	63.24	11.42 (94.6%)[a)]
	82h	0.94	18.96	62.73	11.18 (92.6%)[a)]
	100h	0.93	18.67	62.60	10.87 (90.1%)[a)]

a) The value in parentheses is relative to the initial PCE.

Table S12. The statistical data for optimized device based on PBDB-T:CZTT-IC, PM6:CZTT-IC, PBDB-T:CZTT-4F and PM6:CZTT-4F with different light aging time under continuous illumination in the glove box.

Active Layer	Light Aging Time	V_{OC} (V)	J_{SC} (mA cm-2)	FF (%)	PCE (%)
PBDB-T: CZTT-IC	0h	0.97	17.19	59.12	9.85
	9h	0.97	16.15	58.38	9.14 (92.8%)[a)]
	23h	0.97	14.46	57.96	8.13 (82.5%)[a)]
	40h	0.96	13.64	56.91	7.45 (75.6%)[a)]
	54h	0.95	13.02	53.80	6.65 (67.5%)[a)]
	70h	0.95	12.95	52.57	6.47 (65.7%)[a)]
	100h	0.94	12.12	49.02	5.58 (56.6%)[a)]
PM6: CZTT-IC	0h	1.07	13.14	50.87	7.15
	9h	1.07	12.60	49.41	6.66 (93.1%)[a)]
	23h	1.05	12.06	48.31	6.12 (85.6%)[a)]
	40h	1.05	11.65	45.94	5.62 (78.6%)[a)]
	54h	1.04	10.74	45.22	5.05 (70.6%)[a)]
	70h	1.04	10.34	43.65	4.69 (65.6%)[a)]
	100h	1.04	9.56	43.03	4.28 (59.9%)[a)]
PBDB-T: CZTT-4F	0h	0.88	18.84	58.96	9.77
	9h	0.88	18.76	56.82	9.38 (96.0%)[a)]
	23h	0.87	18.09	54.98	8.65 (88.5%)[a)]
	40h	0.86	17.06	54.29	7.97 (81.6%)[a)]
	54h	0.86	16.69	52.78	7.58 (77.6%)[a)]
	70h	0.86	14.98	48.85	6.29 (64.4%)[a)]
	100h	0.86	14.74	47.99	6.08 (62.2%)[a)]
PM6: CZTT-4F	0h	0.94	19.69	64.98	12.03
	9h	0.94	19.59	64.18	11.82 (98.3%)[a)]
	23h	0.93	18.84	61.97	10.86 (90.3%)[a)]
	40h	0.93	18.68	60.57	10.52 (87.4%)[a)]
	54h	0.93	18.26	59.34	10.08 (83.8%)[a)]
	70h	0.93	17.95	58.28	9.73 (80.9%)[a)]
	100h	0.93	17.67	57.64	9.47 (78.7%)[a)]

a) The value in parentheses is relative to the initial PCE.

Table S13. Summary of carbazole-based devices for binary OSCs in the literature.

Entries	Acceptor	Donor	V_{OC} (V)	J_{SC} (mA cm^{-2})	FF	PCE (%)	Ref.
1	Cz-RH	P3HT	1.03	4.69	0.53	2.56	[13]
2	Cz-IN	P3HT	0.61	0.13	0.26	0.02	[13]
3	Cz-ECA	P3HT	1.00	2.34	0.44	1.03	[13]
4	N7	P3HT	1.17	3.16	0.62	2.30	[14]
5	CBM	PTB7-Th	0.88	10.6	0.53	5.3	[15]
6	DTCC-IC	PTB7-Th	0.95	11.23	0.562	6.0	[16]
7	DTPC-IC	PTB7-Th	0.863	8.53	0.424	3.12	[17]
8	DTPC-DFIC	PTB7-Th	0.760	21.92	0.613	10.21	[17]
9	ICz-Rd_2	P	1.04	14.04	0.54	7.88	[18]
10	ICz-$RdCN_2$	P	1.01	15.58	0.62	9.76	[18]
11	CDTCN	PBDB-T	0.96	11.26	0.576	6.23	[19]
12	DTCCIC-C17	PBDB-T	0.970	14.27	0.678	9.48	[20]
13	DTC-IC	PTB7-Th	0.86	14.12	0.557	7.02	[21]
14	DTC(4Ph)-IC	J71	0.96	13.81	0.585	7.76	[22]
15	DTC(4R)-IC	J71	0.94	16.44	0.620	9.61	[22]
16	DTC(4R)-4FIC	J71	0.82	18.92	0.702	10.89	[22]
17	HCN-C8	J71	1.01	6.24	0.378	2.38	[23]
18	HCN-C16	J71	1.03	12.30	0.435	5.51	[23]
19	H2FCN-C16	J71	0.90	18.62	0.667	11.18	[23]
20	**CZTT-IC**	**PBDB-T**	**0.97**	**17.26**	**0.590**	**9.87**	**This work**
21	**CZTT-IC**	**PM6**	**1.07**	**12.83**	**0.512**	**7.02**	**This work**
22	**CZTT-4F**	**PBDB-T**	**0.88**	**19.06**	**0.585**	**9.81**	**This work**
23	**CZTT-4F**	**PM6**	**0.94**	**19.73**	**0.651**	**12.07**	**This work**

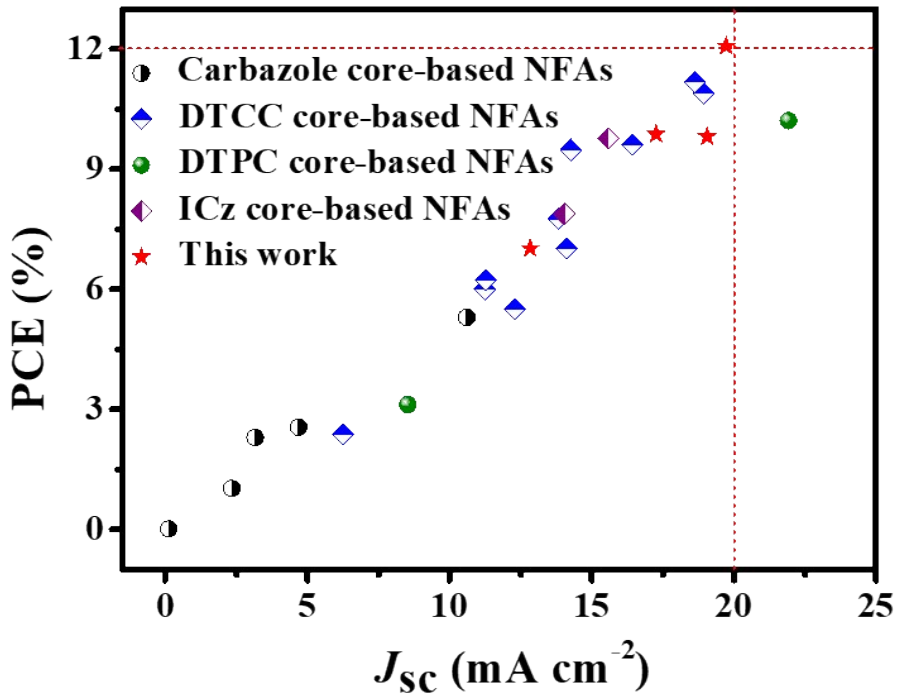

Fig.S27. Summary of J_{SC} and PCE of carbazole-based OSCs in the literature.

Reference

1. W. Zhao, D. Qian, S. Zhang, S. Li, O. Inganas, F. Gao and J. Hou, *Adv Mater.*, 2016, **28**, 4734-4739.
2. B. Guo, W. Li, X. Guo, X. Meng, W. Ma, M. Zhang and Y. Li, *Adv Mater.*, 2017, **29**,1702291.
3. S. Li, L. Zhan, F. Liu, J. Ren, M. Shi, C. Z. Li, T. P. Russell and H. Chen, *Adv Mater.*, 2018, **30**,1705208.
4. H. Cha, J. Wu, A. Wadsworth, J. Nagitta, S. Limbu, S. Pont, Z. Li, J. Searle, M. F. Wyatt, D. Baran, J. S. Kim, I. McCulloch and J. R. Durrant, *Adv Mater.*, 2017, **29**,1701156.
5. Z. Zhang, J. Miao, Z. Ding, B. Kan, B. Lin, X. Wan, W. Ma, Y. Chen, X. Long, C. Dou, J. Zhang, J. Liu and L. Wang, *Nat. commun.*, 2019, **10**, 3271.
6. Z. Wang, Y. Nian, H. Jiang, F. Pan, Z. Hu, L. Zhang, Y. Cao and J. Chen, *Org. Electron.*, 2019, **69**, 174-180.
7. Z. Liu and N. Wang, *Nanoscale*, 2018, **10**, 19524-19535.
8. Y. Gong, K. Chang, C. Chen, M. Han, X. Zhan, J. Min, X. Jiao, Q. Li and Z. Li, *Mater Chem Front.*, 2019, **3**, 93-102.
9. J. Guo, H. Bin, W. Wang, B. Chen, J. Guo, R. Sun, Z.-G. Zhang, X. Jiao, Y. Li and J. Min, *J. Mater. Chem. A*, 2018, **6**, 15675-15683.
10. Y. J. Kim, D. S. Chung and C. E. Park, *Nano Energy*, 2015, **15**, 343-352.
11. L. Zhan, S. Li, S. Zhang, X. Chen, T. K. Lau, X. Lu, M. Shi, C. Z. Li and H. Chen, *ACS Appl Mater Interfaces*, 2018, **10**, 42444-42452.

12. Y. Xin, G. Zeng, J. Ouyang, X. Zhao and X. Yang, *J. Mater. Chem. C*, 2019, **7**, 9513-9522.
13. Y. Kim, C.E. Song, S.-J. Moon, E. Lim, *RSC Adv.*, 2015, **5**, 62739-62746.
14. A.M. Raynor, A. Gupta, H. Patil, D. Ma, A. Bilic, T.J. Rook, S.V. Bhosale, *RSC Adv.*, 2016, **6**, 28103-28109.
15. K. Wang, Y. Firdaus, M. Babics, F. Cruciani, Q. Saleem, A. El Labban, M.A. Alamoudi, T. Marszalek, W. Pisula, F. Laquai, P.M. Beaujuge, *Chem. Mater.*, 2016, **28**, 2200-2208.
16. Q. Cao, W. Xiong, H. Chen, G. Cai, G. Wang, L. Zheng, Y. Sun, *J. Mater. Chem. A*, 2017, **5**, 7451-7461.
17. Z. Yao, X. Liao, K. Gao, F. Lin, X. Xu, X. Shi, L. Zuo, F. Liu, Y. Chen, A.K. Jen, *J. Am. Chem. Soc.*, 2018, **140**, 2054-2057.
18. S. Suman, A. Siddiqui, M.L. Keshtov, G.D. Sharma, S.P. Singh, *J. Mater. Chem. C*, 2019, **7**, 543-552.
19. J. Wei, Q. Tu, Q. Zheng, *Dyes Pigments*, 2017, **144**, 133-141.
20. Y.T. Hsiao, C.H. Li, S.L. Chang, S. Heo, K. Tajima, Y.J. Cheng, C.S. Hsu, *ACS Appl. Mater. Interfaces*, 2017, **9**, 42035-42042.
21. W. Guo, B. Zhao, J. Xin, H. Liu, Y. Mi, J. Zhang, Z. Guo, W. Wei, W. Ma, C. Gao, Z. An, *Dyes Pigments*, 2017, **144**, 48-57.
22. T.-W. Chen, Y.-T. Hsiao, Y.-W. Lin, C.-C. Chang, W.-T. Chuang, Y. Li, C.-S. Hsu, *Mater. Chem. Front.*, 2019, **3**, 829-835.
23. Q. Tu, Y. Ma, X. Zhou, W. Ma, Q. Zheng, *Chem. Mater.*, 2019, DOI: 10.1021/acs.chemmater.9b02355.